

RGO/MXENE INKS FOR EMBEDDED SENSING IN FRP COMPOSITES

D. Anchalee¹, Z. Hanmo², W. Qingqing³ and Z. Limin⁴

¹ School of System Design and Intelligent Manufacturing, Southern University of Science and Technology, Nanshan District, Shenzhen, China, anchalee@sustech.edu.cn

² Department of Applied Physics, The Hong Kong Polytechnic University, Hung Hom, Kowloon, Hong Kong, 20059677r@connect.polyu.hk

³ Department of Mechanical Engineering, The Hong Kong Polytechnic University, Hung Hom, Kowloon, Hong Kong, 22039189r@connect.polyu.hk

⁴ School of System Design and Intelligent Manufacturing, Southern University of Science and Technology, Nanshan District, Shenzhen, China, zhoulm@sustech.edu.cn

Keywords: Nanocomposites, Graphene, MXene, Ultrasonic test

ABSTRACT

This study presents the development and characterization of nonintrusive reduced graphene oxide/MXene (GM) sensors embedded within Fiber Reinforced Polymer (FRP) laminates. The GM sensors, fabricated using non-polymer GM ink with optimized formulation, demonstrate exceptional sensing capabilities and performance. The ink's sensitivity is carefully tuned to ensure its successful integration into FRP laminates without compromising their interlaminar shear stress (ILSS) properties. The integrated GM sensors exhibit an extraordinarily high gauge factor, along with remarkable reversibility and repeatability in responding to dynamic strains. The hybrid functionality achieved by combining GM sensors with GFRP composites offers a unique combination of superior mechanical properties and strain-sensing capabilities. This breakthrough opens up exciting possibilities for a wide range of applications, as FRPs can now provide enhanced structural integrity while simultaneously monitoring and measuring strains with precision.

1 INTRODUCTION

Fiber-reinforced polymer composites (FRPs) have been widely employed in critical engineering applications due to their design flexibility and impressive mechanical properties. To enable continuous and spontaneous monitoring of load-bearing FRPs, various sensors such as optical fiber sensors [1], piezoresistive sensors [2, 3], and lead zirconate titanate (PZT) sensors [4] have been developed. The integration techniques used to combine these sensors with the host structure play a significant role in achieving a robust smart composite. While surface mounting is commonly used for its ease of installation, disassembly, replacement, and maintenance, it exposes the sensors to harsh environmental conditions, potentially leading to failure from chemical corrosion and external impacts over extended operational periods. However, surface mounting is still preferred when convenience, ease of maintenance, and low replacement cost are the primary considerations, even though it may result in inferior signal acquisition accuracy due to direct exposure to the environment and susceptibility to ambient noise

Alternatively, embedding sensors within FRPs can enhance their stability and lifespan addressing the aforementioned issues, especially in harsh environments. Nevertheless, this approach may compromise the original integrity of the host composite structures. PZT sensors, which can be internally embedded into composite structures, have been used for monitoring composites [5, 6], but stress concentration often occurs at the embedded position due to inconsistent material stiffness, impacting the performance and service life of the structure [7]. High sensitivity and mechanical stability of strain gauges are commonly embedded in FRPs to monitor the curing process. Nonetheless, the poor compatibility of strain gauges and wires with epoxy resin can result in delamination after fatigue loading at the embedded position, thus affecting the life of the composite material [8]. These types of sensors are unsuitable for embedding into FRP composites.

Recently, piezoresistive nanocomposite sensors [9-11] have gained popularity for monitoring FRP composite structures due to their higher sensitivities and flexibility compared to conventional strain gauges. Carbonaceous-based sensors have been embedded in FRPs for in-situ curing monitoring and lifelong structural health monitoring [12, 13]. Among various nanofillers, graphene nanoplatelets (GNPs) and MXene have shown promise for nanocomposite sensors due to their ability to form dense and conductive pathways at low nanofiller content resulting in a greater probability of generating the tunnelling effect between adjacent nanoplatelets due to their two-dimensional structure [14, 15]. Implantable graphene/epoxy sensor films have been fabricated with high gauge factors, capable of capturing structural responses up to 600 kHz [16]. Monastyreckis et al. [17] reported a gauge factor of 10.88 at a strain of 4% using an MXene/epoxy-coated sensor on large GFRP composite structures, whereas it exhibited poor stability under tensile cycling loading. However, challenges such as debonding in the interlaminar regions and inhomogeneous dispersion of nanomaterials can compromise the mechanical performance and structural integrity. The restacking and agglomeration of graphene and MXene nanosheets, driven by strong interplanar van der Waals forces and hydrogen bonds, can be overcome by using graphene oxide (GO) instead of graphene and by constructing 3D porous hydrogels. Due to the abundant oxygenate groups with hydrophilicity in GO, it can be chemically reduced to form a conductive reduced graphene oxide (rGO) porous structure for piezoresistive sensors, while retaining the properties of graphene [18]. Although many rGO and MXene-based sensors [19, 20] exhibit excellent flexibility and sensitivity, their low detection range, unstable network structure under cyclic loading, and poor sensing of mechanical signals at high frequencies, such as acoustic-ultrasonic wave-induced strains, significantly restrict their practical applications in the sensing field. Nanocomposite sensors, fabricated using nanofillers and a polymer matrix, often sacrifice the overall mechanical properties of the host FRP laminates due to the incompatible matrix and sensor thickness. Thus, the key challenges in developing nonpolymer-based rGO/MXene (GM) sensors lie in the formulation of inks that can be effectively embedded into FRP composites under noninvasive conditions, with the assistance of the host prepreg epoxy.

To address the aforementioned limitations regarding structural incompatibility between embedded sensors and the host structure, this study focuses on fabricating high-performance sensors using a novel nonpolymer GM ink and subsequently embedding them into FRP composites. The characteristic of GM ink and sensors were thoroughly characterized. The embedded sensors in FRP composites have demonstrated exceptional sensing performance without compromising the original integrity of the composites.

2 MATERIALS AND METHODS

A novel type of piezoresistive nanocomposite sensor has been developed using a cost-effective manufacturing approach involving nonpolymer GM ink. The graphene oxide (GO, >98 wt%, lateral size: > 50 μm), was obtained from TIMESNANO Chengdu. To achieve a uniform dispersion solution, separate dispersions of GO and MXene were prepared in deionized water at concentrations of 1 $\text{mg}\cdot\text{mL}^{-1}$ and 6 $\text{mg}\cdot\text{mL}^{-1}$, respectively, utilizing an ultrasonic bath for a duration of 30 minutes. The MXene solution and L-cysteine were introduced into the GO solution while utilizing a magnetic stirrer at a speed of 1000 rpm for 30 minutes. The resulting suspension was subjected to heating at 95 $^{\circ}\text{C}$ for 6 hours to facilitate the formation of hydrogels. These hydrogels underwent repeated washing with deionized water until reaching a neutral state, after which they were redispersed in DI water through magnetic stirring for 24 hours to produce the GM ink.

The plain weave glass fiber prepregs containing 38 wt% epoxy resin for GFRP composite were sourced from Easycomposites UK. The glass epoxy prepregs were stacked together to create 4-layer FRP composites. Precisely positioned metal wires were used as connecting wires on the first glass fiber prepreg ply, with an electrode distance of 5 mm between the two wires of each sensor. The GM ink was carefully deposited at a specific position where the wires were securely fixed, and a mold was employed to control the initial thickness and shape of the sensor. Once the sensor filled the mold, it was peeled off, and the remaining three prepreg plies were stacked on top. The prepregs, now embedded with sensors, were then subjected to curing at 120 $^{\circ}\text{C}$ for 90 minutes.

3 RESULTS AND DISCUSSION

3.1 Characterizations of GM films

The rheological properties of GM ink were investigated to understand the relationship between ink concentration and viscosity. The viscosity of the non-polymer GM ink was measured using a rheometer (HAAKE MARS 40), and it was observed that the viscosity decreased significantly with increasing shear rate. At a low shear rate of 1 s^{-1} , the viscosity was $0.95 \text{ Pa}\cdot\text{s}$ for a concentration of 30 mg/ml and $0.28 \text{ Pa}\cdot\text{s}$ for 15 mg/ml , as shown in Fig. 1a. Furthermore, the storage (G') and loss moduli (G'') of the ink were analyzed to determine the linear elastic deformation regions and fluidization of the ink network. Fig. 1b shows that the 15 mg/ml concentration exhibited lower storage and loss moduli (9 Pa and 2 Pa , respectively) compared to the 30 mg/ml concentration. The G' and G'' of the 15 mg/ml ink concentration were approximately one order of magnitude lower than those of the 30 mg/ml ink concentration. It is worth noting that the viscosity, storage moduli, and loss moduli of the 30 mg/ml ink were higher than that of the 15 mg/ml ink concentration, primarily due to colloidal and viscous forces. The higher moduli observed at 30 mg/ml , particularly the significantly higher storage modulus, indicate a stiffer and more elastic film structure.

The morphology of the GM film was examined using scanning electron microscopy (SEM, MERLIN), as depicted in Fig. 1c. X-ray diffraction (XRD, Empyrean) analysis confirmed the successful reduction of graphene oxide (GO) to reduced graphene oxide (rGO) and its integration with MXene, as shown in Fig. 1d. The XRD pattern of GO exhibited a sharp peak at approximately 10.7° , corresponding to a d-spacing of 0.83 nm for the 002 planes. An additional peak appeared at 9.1° in the XRD spectra, corresponding to the 002 planes of the MXene (Ti_3C_2) film. In the GM pattern, the 002 peak of GO disappeared, and a broad peak around 22.4° was observed. The broader diffraction peak shifted to higher angles due to the increased interlayer correlation resulting from the intercalation of oxygen functional groups in the interlayer of the rGO lamellae reduced by L-cysteine. The GM pattern exhibited a slight shift towards a lower angle compared to that of rGO, confirming the expansion of the interlayer spacing of the reduced GO flakes through Ti_3C_2 integration.

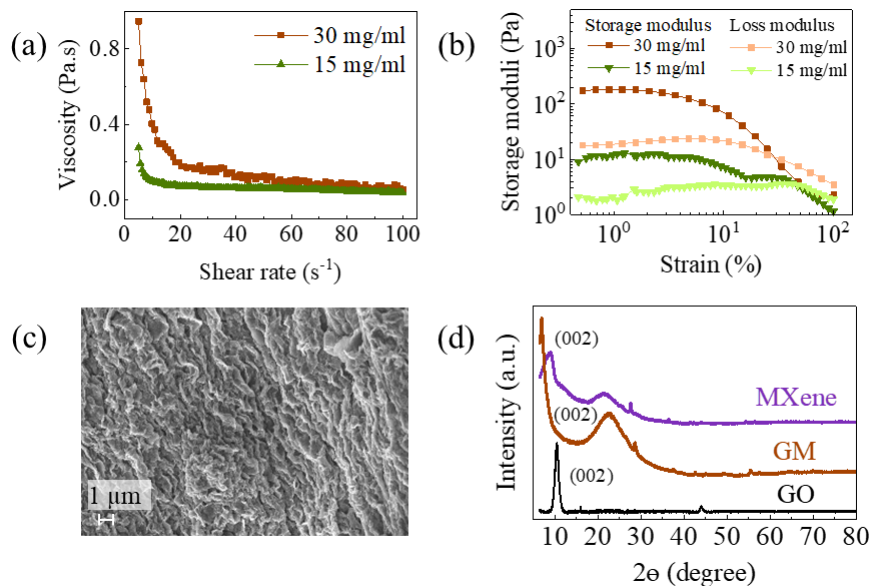


Figure 1: Characterization of GM ink and GM film: (a) Viscosity plotted as a function of the shear rate of GM ink, (b) Storage and loss moduli plotted of GM ink, (c) SEM image of GM film and (d) XRD patterns of GO, GM, and MXene films.

3.2 Mechanical Properties

To assess the compatibility of the GM sensor with composite structures, interlaminar shear stress (ILSS) tests were conducted on composites with and without sensor embedment. Fig. 2 illustrates the ILSS–strain curves of the FRP composites with and without sensor embedment, with FRP laminates without sensor integration serving as a reference. The results indicate that the embedded sensor had a negligible effect on the ILSS of the host laminate structures.

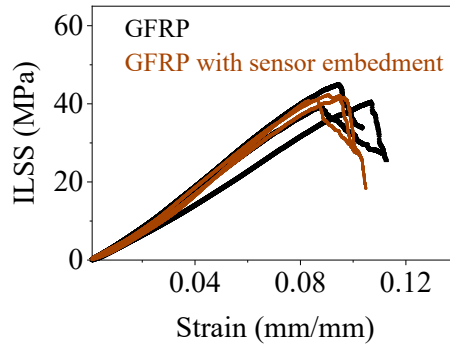


Figure 2: ILSS–strain curves of FRP composites with and without sensor embedment.

3.3 Sensing Performances

Sensitivity is a crucial requirement for sensors used in smart composite structures, particularly for detecting subtle motions or weak signals. The sensitivity of the sensor was investigated through a quasi-static tensile test of GFRP composite integrated with the GM sensor (250 mm × 25 mm). Changes in electrical resistance were measured using a digital multimeter (Keithley® DMM7510) employing the two-point method. The gauge factor (GF), defined as the relative change in electrical resistance due to mechanical strain, was calculated using Equation (1).

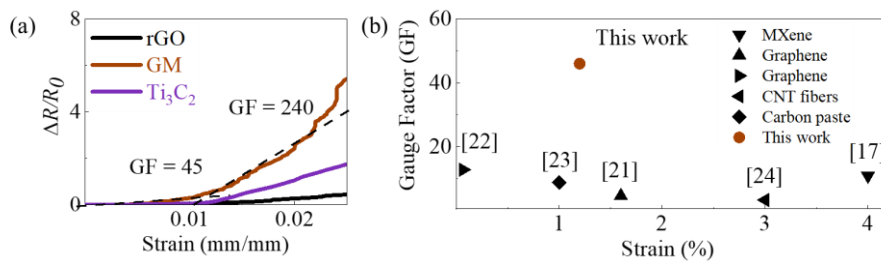


Figure 3. Electromechanical performances of embedded sensors in composites in the quasi-static tensile test: (a) Comparison of the relative change in electrical resistance of the GM sensor with rGO and MXene sensors, and (b) Comparison of the GF of the embedded sensor with other previously published papers [17, 21–24].

Fig. 3a presents the relationship between the relative change in resistance and strain for the embedded GM sensor in the GFRP composite. The changes in resistance can be attributed to modifications in contact resistance caused by the disruption of conductivity paths and variations in the contact area between rGO/MXene nanosheets, leading to an increased tunneling effect between adjacent rGO and MXene. The nanocomposite sensors, leveraging the quantum tunneling effect, exhibited sufficient sensitivity to dynamic strains across a broad range, encompassing static tensile loads with a gauge factor

of 45. A comparison of strain-sensing performances (Fig. 3b) reveals that the GM sensor's sensing performance is highly competitive with those reported in previous studies indicated that the GM sensor performed competitively [17, 21-24].

$$GF = (\Delta R/R_0)/\varepsilon \quad (1)$$

where ΔR is the change in electrical resistance, R_0 is the initial resistance, and ε is the tensile strain.

The long-term sensing stability of the embedded sensor in FRPs (250 mm × 25 mm × 0.87 mm) was examined through cyclic tensile tests at a frequency of 1 Hz for 6,000 cycles using an electrodynamic testing machine (ZwickRoell® linear testing system 10 kN), as depicted in Fig. 4a. The resistance of the sensor remained unchanged, indicating excellent durability and reliability of the GM sensors due to the synergistic effect of rGO and MXene. These cyclic results demonstrate the reliability and stability of the GM sensor, which can be attributed to the homogeneous dispersion of the GM ink.

For the ultrasonic test, a GFRP (250 mm × 250 mm × 0.87 mm) with the embedded sensor was prepared, and a PZT wafer (PSN-33, Ø10 mm, 1 mm thick) was surface-mounted on it. A 3-cycle Hanning-window-modulated sinusoidal tone burst with a central frequency of 150 kHz was generated by a waveform generator (Tektronix® AFG31051), and then amplified using a power amplifier (Falco systems® WMA-300) to excite the PZT wafer. Another receiving PZT wafer was mounted on the surface where the GM sensor was embedded, 100 mm away from the excited PZT, to calibrate and compare the signals acquired by both sensors. Filtered ultrasonic signals acquired with the GM sensor and PZT wafer at 150 kHz are shown in Fig. 4b. The arrival time of the first arrival zeroth-order symmetric Lamb wave (S_0) exhibited qualitative coincidence between the signals acquired by the PZT and the embedded GM sensor for the wave modes. The arrival times of the GM sensors were almost coincident and in good agreement with the PZT wafer. Discrepancies in signal magnitude captured by the two types of sensors can be attributed to their distinct sensing mechanisms. The PZT wafer measures changes in piezoelectricity, whereas the nanocomposite sensor detects variations in piezoresistive properties based on the tunneling effect. The captured signals of the embedded sensor exhibited a negligible lag in arrival time compared to the PZT wafer, indicating good sensitivity and reliability at high frequencies.

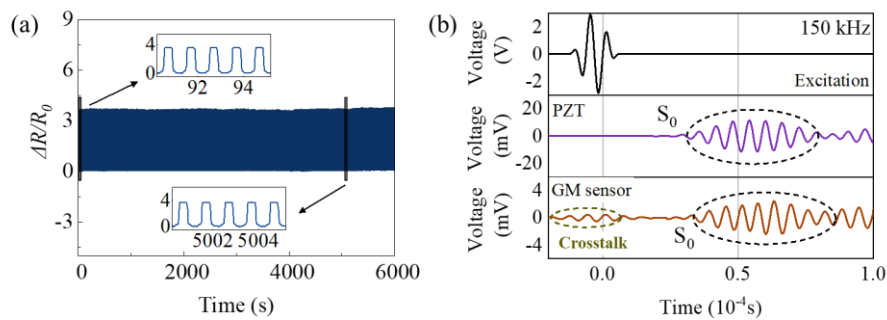


Figure 4. Electromechanical performances of embedded sensors in composite: (a) Change in electrical resistance of the embedded sensor during cyclic strain at 1 Hz for 6,000 cycles, and (b) Ultrasonic wave signals acquired with the embedded GM sensor and surface-mounted PZT wafer at 150 kHz.

4 CONCLUSIONS

In conclusion, the characterizations and performance evaluations presented in this study provide valuable insights into the properties and capabilities of the GM sensor for FRP composite structures. The characterizations of GM films underscore the importance of ink concentration, film microstructure, and the successful integration of GO and MXene in achieving the desired properties of the GM films. The mechanical compatibility of the GM sensor with composite structures was assessed through ILSS tests, demonstrating that the integration of the GM sensor does not compromise the mechanical integrity

of the composites. This finding is crucial for the practical application of the GM sensor in FRP composite structures. Furthermore, the quasi-static tensile test reveals its sensitivity to mechanical strain, with a high gauge factor indicating accurate strain measurement even at low magnitudes. The long-term sensing stability tests demonstrated the excellent durability and reliability of the GM sensor due to the homogeneous dispersion of the sensing material. The GM sensor's ability to detect ultrasonic waves was evaluated and compared to a traditional PZT wafer. The GM sensor exhibited qualitative agreement with the PZT wafer in terms of time-of-flight measurements, highlighting its potential for wave mode detection. The distinct sensing mechanisms of the GM sensor, based on piezoresistive properties, contributed to its sensitivity and reliability at high frequencies. Overall, the results emphasize the promising characteristics and performance of the GM sensor, making it a viable candidate for integration into composite structures. Its compatibility with composites, high sensitivity to mechanical strain, long-term stability, and potential for ultrasonic wave detection highlight its potential applications in various industries. Further research and development of the GM sensor could lead to advancements in the field of smart composite materials, enabling the development of robust and multifunctional structures with enhanced sensing capabilities.

ACKNOWLEDGEMENTS

This research was supported by the National Natural Science Foundation of China [Grant No. 12072141]

REFERENCES

- [1] O. Rufai, N. Chandarana, M. Gautam, P. Potluri, M. Gresil, Cure monitoring and structural health monitoring of composites using micro-braided distributed optical fibre, *Composite Structures* **254** (2020) 112861 (doi: [10.1016/j.compstruct.2020.112861](https://doi.org/10.1016/j.compstruct.2020.112861)).
- [2] H. Dong, H. Liu, A. Nishimura, Z. Wu, H. Zhang, Y. Han, T. Wang, Y. Wang, C. Huang, L. Li, Monitoring strain response of epoxy resin during curing and cooling using an embedded strain gauge, *Sensors* **21**(1) (2020) 172.
- [3] M. Bhandari, J. Wang, D. Jang, I. Nam, B. Huang, A Comparative Study on the Electrical and Piezoresistive Sensing Characteristics of GFRP and CFRP Composites with Hybridized Incorporation of Carbon Nanotubes, Graphenes, Carbon Nanofibers, and Graphite Nanoplatelets, *Sensors (Basel)* **21**(21) (2021) 7291 (10.3390/s21217291).
- [4] H. Alnuaimi, U. Amjad, P. Russo, V. Lopresto, T. Kundu, Monitoring damage in composite plates from crack initiation to macro-crack propagation combining linear and nonlinear ultrasonic techniques, *Structural Health Monitoring* **20**(1) (2021) 139-150 (doi: [10.1177/1475921720922922](https://doi.org/10.1177/1475921720922922)).
- [5] S. Masmoudi, A. El Mahi, S. Turki, Fatigue behaviour and structural health monitoring by acoustic emission of E-glass/epoxy laminates with piezoelectric implant, *Applied Acoustics* **108** (2016) 50-58 (10.1016/j.apacoust.2015.10.024).
- [6] C. Andreades, P. Mahmoodi, F. Ciampa, Characterisation of smart CFRP composites with embedded PZT transducers for nonlinear ultrasonic applications, *Composite Structures* **206** (2018) 456-466 (doi: [10.1016/j.compstruct.2018.08.083](https://doi.org/10.1016/j.compstruct.2018.08.083)).
- [7] H.P. Konka, M. Wahab, K. Lian, The effects of embedded piezoelectric fiber composite sensors on the structural integrity of glass-fiber-epoxy composite laminate, *Smart materials and Structures* **21**(1) (2011) 015016).
- [8] M. Kanerva, P. Antunes, E. Sarlin, O. Orell, J. Jokinen, M. Wallin, T. Brander, J. Vuorinen, Direct measurement of residual strains in CFRP-tungsten hybrids using embedded strain gauges, *Materials & Design* **127** (2017) 352-363 (doi: [10.1016/j.matdes.2017.04.008](https://doi.org/10.1016/j.matdes.2017.04.008)).
- [9] Y. Li, K. Wang, Z. Su, Dispersed Sensing Networks in Nano-Engineered Polymer Composites: From Static Strain Measurement to Ultrasonic Wave Acquisition, *Sensors* **18**(5) (2018) (doi: [10.1088/0964-1726/21/1/015016](https://doi.org/10.1088/0964-1726/21/1/015016)).
- [10] P. Zhou, Y. Liao, Y. Li, D. Pan, W. Cao, X. Yang, F. Zou, L.-m. Zhou, Z. Zhang, Z. Su, An inkjet-printed, flexible, ultra-broadband nanocomposite film sensor for in-situ acquisition of

- high-frequency dynamic strains, *Composites Part A: Applied Science and Manufacturing* **125** (2019) 105554 (doi: [10.1016/j.compositesa.2019.105554](https://doi.org/10.1016/j.compositesa.2019.105554)).
- [11] Z. Zeng, M. Liu, H. Xu, Y. Liao, F. Duan, L.-m. Zhou, H. Jin, Z. Zhang, Z. Su, Ultra-broadband frequency responsive sensor based on lightweight and flexible carbon nanostructured polymeric nanocomposites, *Carbon* **121** (2017) 490-501 (doi: [10.1016/j.carbon.2017.06.011](https://doi.org/10.1016/j.carbon.2017.06.011)).
- [12] S. Luo, T. Liu, Graphite nanoplatelet enabled embeddable fiber sensor for in situ curing monitoring and structural health monitoring of polymeric composites, *ACS Applied Materials and Interfaces* **6**(12) (2014) 9314-9320 (doi: [10.1021/am5017039](https://doi.org/10.1021/am5017039)).
- [13] S. Luo, G. Wang, Y. Wang, Y. Xu, Y. Luo, Carbon nanomaterials enabled fiber sensors: A structure-oriented strategy for highly sensitive and versatile in situ monitoring of composite curing process, *Composites Part B: Engineering* **166** (2019) 645-652 (doi: [10.1016/j.compositesb.2019.02.067](https://doi.org/10.1016/j.compositesb.2019.02.067)).
- [14] A. Nag, A. Mitra, S.C. Mukhopadhyay, Graphene and its sensor-based applications: A review, *Sensors and Actuators A: Physical* **270** (2018) 177-194 (doi: [10.1016/j.sna.2017.12.028](https://doi.org/10.1016/j.sna.2017.12.028)).
- [15] K. Grabowski, S. Srivatsa, A. Vashisth, L. Mishnaevsky, T. Uhl, Recent advances in MXene-based sensors for Structural Health Monitoring applications: A review, *Measurement* **189** (2022) 110575 (doi: [10.1016/j.measurement.2021.110575](https://doi.org/10.1016/j.measurement.2021.110575)).
- [16] Q. Wang, Y. Tian, A. Duongthiphewa, J. Zhang, M. Liu, Z. Su, L. Zhou, An embedded non-intrusive graphene/epoxy broadband nanocomposite sensor co-cured with GFRP for in situ structural health monitoring, *Composites Science and Technology* **236** (2023) 109995 (doi: [10.1016/j.compscitech.2023.109995](https://doi.org/10.1016/j.compscitech.2023.109995)).
- [17] G. Monastyreckis, A. Stepura, Y. Soyka, H. Maltanova, S.K. Poznyak, M. Omastová, A. Aniskevich, D. Zeleniakiene, Strain Sensing Coatings for Large Composite Structures Based on 2D MXene Nanoparticles, *Sensors* **21**(7) (2021) 2378 (doi: [10.3390/s21072378](https://doi.org/10.3390/s21072378)).
- [18] Q. Li, Y. Liu, D. Chen, J. Miao, S. Lin, D. Cui, Highly Sensitive and Flexible Piezoresistive Pressure Sensors Based on 3D Reduced Graphene Oxide Aerogel, *IEEE Electron Device Letters* **42**(4) (2021) 589-592 (doi: [10.1109/LED.2021.3063166](https://doi.org/10.1109/LED.2021.3063166)).
- [19] M. Zhu, Y. Yue, Y. Cheng, Y. Zhang, J. Su, F. Long, X. Jiang, Y. Ma, Y. Gao, Hollow MXene Sphere/Reduced Graphene Aerogel Composites for Piezoresistive Sensor with Ultra-High Sensitivity, *Advanced Electronic Materials* **6**(2) (2020) 1901064 (doi: [10.1002/aelm.201901064](https://doi.org/10.1002/aelm.201901064)).
- [20] F. Niu, Z. Qin, L. Min, B. Zhao, Y. Lv, X. Fang, K. Pan, Ultralight and Hyperelastic Nanofiber-Reinforced MXene-Graphene Aerogel for High-Performance Piezoresistive Sensor, *Advanced Materials Technologies* **6**(11) (2021) 2100394 (doi: [10.1002/admt.202100394](https://doi.org/10.1002/admt.202100394)).
- [21] M. Anas, M.A. Nasir, Z. Asfar, S. Nauman, M. Akalin, F. Ahmad, Structural health monitoring of GFRP laminates using graphene-based smart strain gauges, *Journal of the Brazilian Society of Mechanical Sciences and Engineering* **40**(8) (2018) 397 (doi: [10.1007/s40430-018-1320-4](https://doi.org/10.1007/s40430-018-1320-4)).
- [22] T.T. Tung, R. Karunagaran, D.N.H. Tran, B. Gao, S. Nag-Chowdhury, I. Pillin, M. Castro, J.-F. Feller, D. Losic, Engineering of graphene/epoxy nanocomposites with improved distribution of graphene nanosheets for advanced piezo-resistive mechanical sensing, *Journal of Materials Chemistry C* **4**(16) (2016) 3422-3430 (doi: [10.1039/C6TC00607H](https://doi.org/10.1039/C6TC00607H)).
- [23] Y. Zhang, N. Anderson, S. Bland, S. Nutt, G. Jursich, S. Joshi, All-printed strain sensors: Building blocks of the aircraft structural health monitoring system, *Sensors and Actuators A: Physical* **253** (2017) 165-172 (doi: [10.1016/j.sna.2016.10.007](https://doi.org/10.1016/j.sna.2016.10.007)).
- [24] N.D. Alexopoulos, C. Bartholome, P. Poulin, Z. Marioli-Riga, Structural health monitoring of glass fiber reinforced composites using embedded carbon nanotube (CNT) fibers, *Composites Science and Technology* **70**(2) (2010) 260-271 (doi: [10.1016/j.compscitech.2009.10.017](https://doi.org/10.1016/j.compscitech.2009.10.017)).